Multiobjective Shape Optimization of Linear Elastic Structures Considering Multiple Loading Conditions*
(Dealing with Mean Compliance Minimization Problems)

Masatoshi SHIMODA**, Hideyuki AZEGAMI***
and Toshiaki SAKURAI**

We describe numerical analysis methods for multiobjective shape optimization of linear elastic structures. As an example, we consider a multiloading mean compliance minimization problem with a volume constraint. The methods presented here are based on the traction method, in which the speed field representing the domain variation is analyzed. A weighted l_p-norm method with four types of norm is employed to scalarize the multiobjective functionals. The shape gradient functions for each scalarized objective functional are obtained using the Lagrange multiplier method. A general-purpose finite element code is used to perform the numerical analyses. Numerical analysis results for a multiply connected plate problem and a solid structure problem under multiloading conditions are presented to demonstrate the validity of the traction method in obtaining Pareto optimal solutions.

Key Words: Optimum Design, Computational Mechanics, Finite Element Method, Structural Analysis, Domain Optimization, Multiobjective Optimization, Pareto Solution, Traction Method, Multiply Connected Domain

1. Introduction

A key concern in structural design is the determination of the optimal shapes of multiobjective structures subject to multiloading conditions efficiently and economically. The term multiloading here refers to a number of loads that act independently on a multiobjective structure. This is a multiobjective optimization involving the determination of Pareto optimal solutions with respect to objective functionals which generally requires trade-offs.

There is a considerable number of reports on shape optimization problems involving a single loading condition[1],[2]. Studies on shape optimization problems involving multiloading conditions, which is the situation that structural designers actually encounter, are limited in number. Most of the structural optimization studies on multiloading conditions have been limited to beam structures; in other words, they have dealt with size optimization problems[3]-[5].

One of the few studies on multiobjective shape optimization problems involving multiloading conditions was reported by Tada et al[6]. They scalarized the objective functions by applying a weighting method to minimize the potential energy of each load and found Pareto solutions to a two-dimensional shape optimization problem using the energy ratio method. In a separate study, Kikuchi found Pareto optimal solutions to a topology optimization problem using an approximation of the min-max method[7].

We, on the other hand, have focused on the traction method[8] for solving shape optimization problems. In previous work, a shape optimization system has been developed which is applicable to problems involving a single loading condition[9]. In the traction method, the domain variation is analyzed numerically

as the displacement field in a pseudoelastic problem subjected to a pseudoforce which is in proportion to the shape gradient function (i.e., the shape sensitivity). This method is practical because the finite element and boundary element methods can be used in performing the numerical analyses. It is also extremely easy to use when a mechanically simple functional such as the mean compliance is selected as the objective functional. Additionally, because domain variation can be analyzed in terms of the variation of the entire domain, the traction method has the advantage that the mesh of internal nodes does not have to be refined when the finite element method is used.

We apply the traction method to multiobjective shape determination problems involving multiloading conditions. The mean compliance of a linear elastic continuum subject to multiloading conditions is selected as the objective functional, which is scalarized using four types of norm determined by the weighted l_p norm method. This functional expresses the mean stiffness relative to the application of multiple loads. Weighting makes it possible to vary the extent to which each load is considered. Numerical analysis results for multiply connected problems in two and three dimensions are presented to demonstrate the effectiveness and utility of the traction method in solving multiobjective shape optimization problems involving multiloading conditions.

2. Mean Compliance Minimization Problem with Multiloading Conditions

As shown in Fig. 1, we assume that a linear elastic continuum with an initial domain $\Omega \subset R^n$ ($n=2, 3$) and boundary $\Gamma \equiv \partial\Omega$ undergoes a variation such that its domain and boundary become Ω_s, and $\Gamma_s \equiv \partial\Omega_s$. The subscript s indicates the history of domain variation. Body forces $f^{(m)}$ and surface forces $P^{(m)}(m=1, 2, \cdots, N)$ are assumed to act on Ω_s and Γ_1, respectively. It is assumed that N loads act on the domain independently. The weighted l_p-norm method is used to scalarize the objective functional[10]. Letting $v^{(m)}$ and $l(v^{(m)}) \equiv l_m$ denote the displacement and mean compliance for the load m, the l_p-norm of the mean compli-

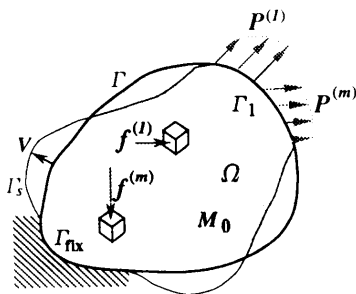Fig. 1 Domain variation problem of elastic continuum

ance $\|l\|_p^c$ is expressed as

$$\|l\|_p^c = \left\{ \sum_{m=1}^{N} (c^{(m)} l(v^{(m)}))^p \right\}^{1/p}, \quad p \in [1, \infty], \quad (1)$$

where $c = (c^{(1)}, c^{(2)}, \cdots, c^{(N)})^T \geq 0$ is a weighting coefficient vector.

The speed method used to describe domain variation is explained elsewhere[8].

2.1 Weighting method (method 1)

Assuming that $p=1$ in Eq. (1), a mean compliance minimization problem with multiloading conditions can be formulated as shown below using the weighting method. In this problem, the equations of state and the volume are given as constraints.

Given Ω, $f^{(m)}$ in Ω, $P^{(m)}$ on Γ_1, e in Ω,

$$M_0 \in R_+, \quad c \in R_+^N \quad (2)$$

find Ω_s (3)

that minimize $\|l\|_1^c$, (4)

subject to $a(v^{(m)}, w^{(m)}) = l(w^{(m)})$ (5)

for all $w^{(m)} \in U$, $m=1, \cdots, N$,

$$M - M_0 \leq 0, \quad (6)$$

here, the bilinear form $a(v^{(m)}, w^{(m)})$ which gives the variational strain energy for the m th load, the linear form $l(w^{(m)})$ which gives the variational potential energy or variational mean compliance due to the applied external force and the volume M are defined as

$$a(v^{(m)}, w^{(m)}) = \int_{\Omega_s} e_{ijkl} v_{k,l}^{(m)} w_{i,j}^{(m)} d\Omega, \quad (7)$$

$$l(w^{(m)}) = \int_{\Omega_s} f_i^{(m)} w_i^{(m)} d\Omega + \int_{\Gamma_1} P_i^{(m)} w_i^{(m)} d\Gamma, \quad (8)$$

$$M = \int_{\Omega_s} dx, \quad (9)$$

where v_i, w_i and e_{ijkl} are displacement, variational displacement and an elastic tensor, respectively. U denotes the space of kinematically admissible displacements. The notation R_+ denotes the set of positive real numbers. Einstein's summation convention is used in the tensor notation in this paper and a partial differential notation $(\cdot)_{,i} = \partial(\cdot)/\partial x_i$ is used. The Lagrangian functional for this problem is expressed as

$$L(\Omega, v^{(1)}, \cdots, v^{(N)}, w^{(1)}, \cdots, w^{(N)}, \Lambda)$$
$$= \sum_{m=1}^{N} \{c^{(m)} l(v^{(m)})\} + \sum_{m=1}^{N} \{l(w^{(m)})$$
$$- a(v^{(m)}, w^{(m)})\} + \Lambda(M - M_0) \quad (10)$$

The following assumptions are made for simplicity: the boundary at which the surface forces act does not vary in the normal direction ($n_i V_i = 0$ on Γ_1), the material is homogeneous and unchanged ($e'_{ijkl} = e_{ijkl} = 0$), and the body forces are constant within a domain ($f' = 0$)[12]. Then, the derivative $\dot{L}$ of the domain variation of the Lagrangian functional L can be expressed as shown below using the speed field V with respect to the domain variation[8].

$$\dot{L} = \sum_{m=1}^{N} \{ c^{(m)} l(v'^{(m)}) - a(v'^{(m)}, w^{(m)}) \}$$

$$+ \sum_{m=1}^{N} \{ l(w'^{(m)}) - a(v^{(m)}, w'^{(m)}) \} + \Lambda'(M - M_0)$$

$$+ \int_{\Gamma_s} \Big\{ \sum_{m=1}^{N} (c^{(m)} f_i^{(m)} v_i^{(m)} + f_i^{(m)} w_i^{(m)} $$

$$- e_{ijkl} v_{k,l}^{(m)} w_{i,j}^{(m)}) + \Lambda \Big\} n_l V_l d\Gamma, \tag{11}$$

where $(:)$ and $(\cdot)'$ indicate a material derivative and a shape derivative, respectively[11].

When v is determined from the state equations,

$$a(v^{(m)}, w'^{(m)}) = l(w'^{(m)}) \text{ for all } w' \in U,$$
$$m = 1, \cdots, N. \tag{12}$$

w from the adjoint equations,

$$a(v'^{(m)}, w^{(m)}) = c^{(m)} l(v'^{(m)})$$
$$\text{for all } v' \in U, m = 1, \cdots, N, \tag{13}$$

and Λ is determined so as to satisfy the Kuhn-Tucker conditions

$$\Lambda(M - M_0) = 0, \tag{14}$$
$$M - M_0 \le 0, \tag{15}$$

Eq. (11) becomes

$$\dot{L} = l_G(V) \tag{16}$$

$$l_G(V) = \int_{\Gamma_s} G_i V_i d\Gamma \tag{17}$$

$$G = \Big[\sum_{m=1}^{N} \{ c^{(m)} (2 f_i^{(m)} v_i^{(m)} - e_{ijkl} v_{k,l}^{(m)} v_{i,j}^{(m)}) + \Lambda \} \Big] n$$
$$\text{on } \Gamma \backslash \Gamma_1 \tag{18}$$

using the relationship between v and w:

$$w^{(m)} = c^{(m)} v^{(m)}, m = 1, \cdots, N. \tag{19}$$

G represents the shape sensitivity and is called the shape gradient function. If the shape gradient function is given, it is possible to use the traction method.

2.2 Weighted min-max method (method 2)

Assuming that $p \to \infty$ in Eq. (1), the problem can be formulated as a multiobjective optimization problem using a weighted min-max method. In this case, the problem is expressed by rewriting Eq. (1) as

$$\underset{\Omega_s}{\text{minimize}} \| l \|_\infty^C = \underset{\Omega_s}{\text{minimize}} \max_{m=1,\cdots,N} \{ c^{(m)} l(v^{(m)}) \}$$
$$\text{at each iteration.} \tag{20}$$

In this method, the problem becomes that of a single load condition at each iteration in relation to the maximum load m. Therefore, the shape gradient function G is given by the following expression which corresponds to Eq. (18):

$$G = \{ c^{(m)} (2 f_i^{(m)} v_i^{(m)} - e_{ijkl} v_{k,l}^{(m)} v_{i,j}^{(m)}) + \Lambda \} n$$
$$\text{for max. load } (m) \text{ on } \Gamma \backslash \Gamma_1. \tag{21}$$

2.3 Normalized weighted min-max method (method 3)

The objective functional is considered as a normalized objective functional

$$\bar{l}(v^{(m)}) = \frac{l(v^{(m)}) - l_{\min}(v^{(m)})}{l_{ini}(v^{(m)}) - l_{\min}(v^{(m)})}. \tag{22}$$

where $l_{ini}(v^{(m)})$ is the mean compliance of the initial shape for load m and $l_{\min}(v^{(m)})$ is the mean compliance

of the optimum shape for a single load m. The method based on Eq. (23) is referred to here as a normalized weighted min-max method.

$$\underset{\Omega_s}{\text{minimize}} \| l \|_\infty^C = \underset{\Omega_s}{\text{minimize}} \max_{m=1,\cdots,N} \{ c^{(m)} \bar{l}(v^{(m)}) \}$$
$$\text{at each iteration.} \tag{23}$$

The shape gradient function G for this problem is given by Eq. (21), as for method 2. Although method 3 is a min-max method similar to method 2, it is intended to take the mean compliance of each load as close as possible to a complete optimal solution. As such, it minimizes the mean compliance of the load at the greatest distance from the complete optimal solution. The problem is thus formulated by a type of compromise programming method. Method 2 provides an absolute evaluation of each objective functional whereas method 3 provides a relative evaluation.

2.4 Weighted minimum localized maximum method (method 4)

By modifying the weighted min-max method, the following method of using G in accordance with the concept of a localized maximum[7] is considered. In this method, the shape gradient function of each load is evaluated locally, and the maximum value obtained is taken as the representative shape gradient function for that part of the structure. Comparison with Eq. (21) indicates that an inequality such as that in Eq. (24) holds true.

$$G = \max_{m=1,\cdots,N} |\{ c^{(m)} (2 f_i^{(m)} v_i^{(m)} - e_{ijkl} v_{k,l}^{(m)} v_{i,j}^{(m)}) \} + \Lambda | n$$

$$(\ge | c^{(m)} (2 f_i^{(m)} v_i^{(m)} - e_{ijkl} v_{k,l}^{(m)} v_{i,j}^{(m)} + \Lambda | n$$
$$\text{for max. load } (m)). \tag{24}$$

This method is referred to as the weighted minimum localized maximum method in this work.

3. Traction Method

The traction method has been proposed as a procedure for obtaining the speed field V, based on the governing equation:

$$a(V, w) = - l_G(w) \text{ for all } w \in c_\theta \tag{25}$$

where c_θ denotes the space of kinematically admissible speeds.

This equation indicates that the speed field V corresponds to a displacement field when the negative shape gradient function $- G$ acts as an external force. This means that Eq. (25) can be solved using a general method for solving linear elastic problems. In this work, the finite element method is used. The shape is updated by multiplying the value of V thus obtained by a coefficient Δs that adjusts the amount of domain variation per iteration. By repeating the stress analysis which yields the shape gradient function, the speed analysis which yields the speed field and the updating of the shape, the objective functional is minimized,

resulting in the optimal shape. A schematic of the traction method is shown in Fig. 2.

Equations (14) and (15) represent the Kuhn-Tucker conditions with respect to the volume constraint. The following concept of volume control is used as a method of satisfying these conditions. The Lagrangian multiplier Λ, determined so as to satisfy the volume constraint, can be regarded as a uniform surface force in the external force $-G$. Therefore, by controlling the magnitude of this uniform surface force Λ, it should be possible to satisfy the conditions of Eqs. (14) and (15). The method used here to control Λ is based on the concept of the proportional-integral-derivative (PID) control. A detailed explanation of the procedure is given elsewhere[9].

In order to apply the traction method to shape optimization problems in actual design work, we have developed a shape optimization system based on a general-purpose finite element code. Experimental application of the system has confirmed its validity in solving problems involving a single load condition[9]. The results obtained in the present study have also been incorporated into the system.

4. Numerical Results

The shape optimization system was applied to multiply connected problems in two and three dimensions to confirm the validity of the above methods, based on the traction method, in solving multiobjective shape optimization problems. In addition, for the two-dimensional problem, the Pareto optimal shapes obtained when shape gradient functions defined by methods 1–4 were used, were compared. The two dimensional problem involved determining the optimal shape of three holes in a plate. The three-dimensional problem involved determining the optimal thickness of a bracket with a semicircular hole. A constant volume (area) was given as a constraint in both problems.

4.1 Two-dimensional problem

The problem is illustrated in Fig. 3. In the stress analysis, one end of the plate was fully restrained and two different load distributions were applied to the other end, as shown in Fig. 3(a). A shear load $P^{(1)}$ was applied in case 1 and a tensile load $P^{(2)}$ was applied in case 2. In the speed analysis, it was assumed that the outer periphery of the plate was subject to a constraint and did not vary, as shown in Fig. 3(b). The design boundary was thus defined as the circumference of the three holes. The weighting coefficient $c^{(1)}$ was varied over five stages from 0.2 to 0.8 and $c^{(2)}$ was defined as $1-c^{(1)}$. A plane stress condition was assumed, and a quadrilateral element with four nodes was used in the numerical analysis.
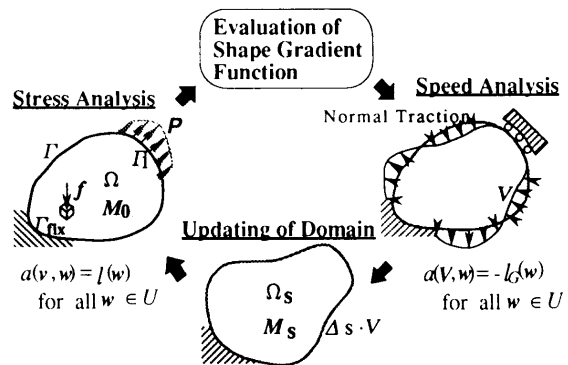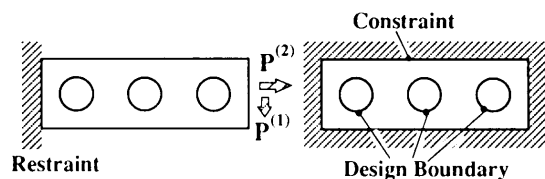

Fig. 2 Schematic of traction method

(a) Stress analysis   (b) Speed analysis

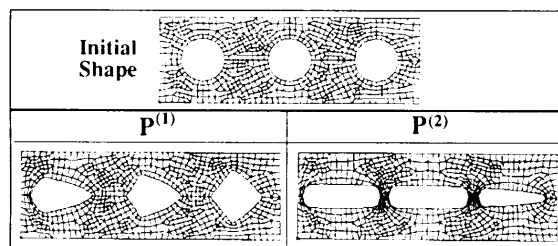Fig. 3 Shape optimization problem for holes in plate

Fig. 4 Initial shape and optimal shape under single loading condition
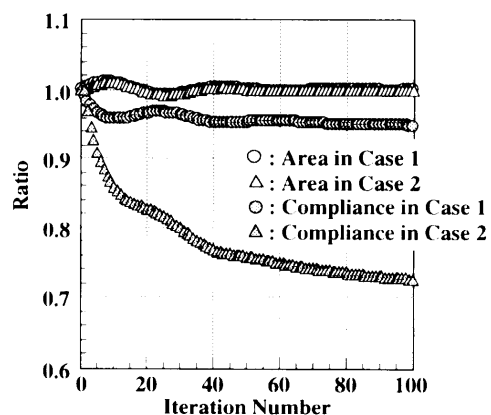

Fig. 5 Iteration histories for single loading condition

Figure 4 shows the initial shape and the optimal shapes computed for the single loads $P^{(1)}$ and $P^{(2)}$ for comparison with the Pareto optimal shapes. Iteration histories of the optimization calculations are shown in Fig. 5. In both cases 1 and 2, the area was controlled so that it remained constant. Compared with the
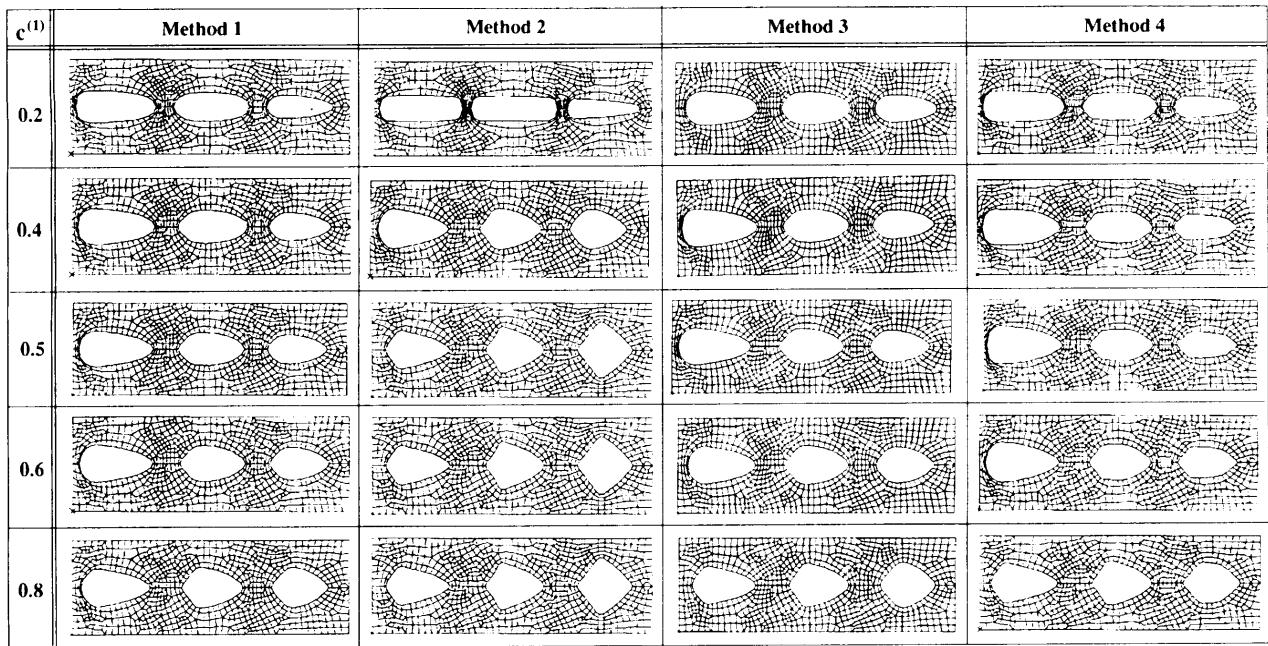
Fig. 6   Pareto optimal shapes under multiloading in two directions
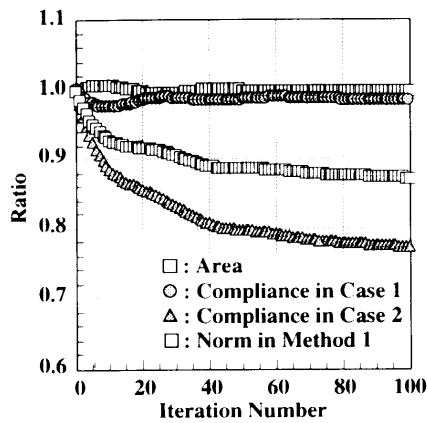

Fig. 7   Iteration histories for method 1 under multiloading in two directions ($c^{(1)}=0.4$)
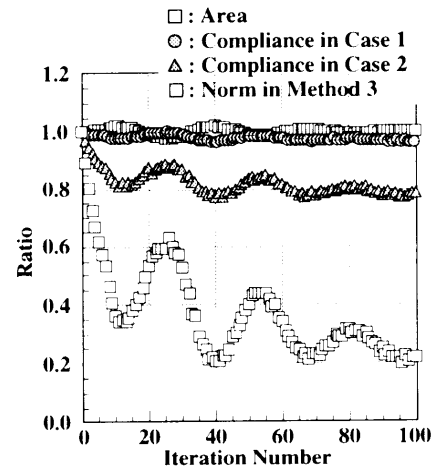

Fig. 9   Iteration histories for method 3 under multiloading in two directions ($c^{(1)}=0.4$)
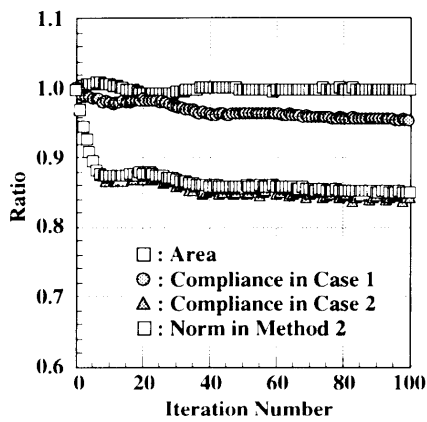

Fig. 8   Iteration histories for method 2 under multiloading in two directions ($c^{(1)}=0.4$)
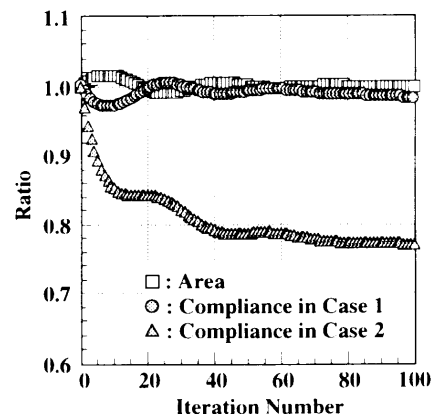

Fig. 10   Iteration histories for method 4 under multiloading in two directions ($c^{(1)}=0.4$)

412

initial shape, the objective functional was reduced by approximately 5% in case 1 and by approximately 27% in case 2.

Figure 6 shows the Pareto optimal shapes obtained when the shape gradient functions defined by methods 1-4 were used. With the exception of method 2, these methods yielded shapes that are quite similar overall, although some localized differences are observed. When $c^{(1)}$ was small, the shape was strongly influenced by $P^{(2)}$. As the value of the weighting coefficient was increased, the shape gradually began to show the influence of $P^{(1)}$. In contrast, it became more difficult to obtain an intermediate shape using method 2.

Figures 7-10 show iteration histories of the optimization calculations performed using methods 1-4, respectively, for multiloading conditions when $c^{(1)}$ was set at 0.4. The results confirm that the area constraint was satisfied with all four methods. The mean compliance and the norm defined by each method were minimized by the final iteration in all four methods, although the intermediate processes differed. As expected with the min-max theory, the iteration histories for methods 2 and 3 in particular show repetitive minimization of maxima.

Figure 11 shows a comparison of the mean compliances obtained using the four methods for each weighting coefficient value. The notations l_1 and l_2 in
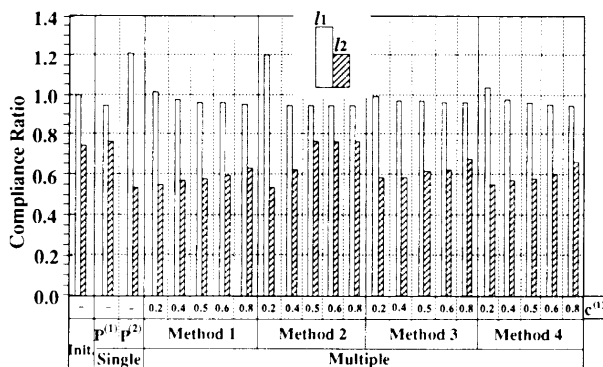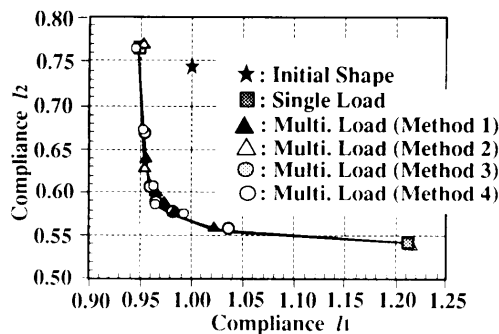
the figure denote the mean compliances for cases 1 and 2, respectively. All of the mean compliances have been normalized by the mean compliance of the initial shape in case 1. Similar to the results shown in Fig. 6, the mean compliances obtained with method 4 agree well with the values obtained using the other methods except for method 2. When $c^{(1)}$ was 0.4 or greater, the mean compliances in both cases 1 and 2 were reduced in comparison with the results for the initial shape.

In Fig. 12, the above results are plotted in an objective functional space which has two objective functionals as its coordinates. The results obtained with the four methods fall almost entirely on the same curve. Excluding method 2, it is clear that a complete set of Pareto optimal shapes can be obtained by varying the weighting coefficient. Obtaining a complete set of the Pareto optimal shapes with method 2 would require finer adjustments of the weighting coefficient (e.g., fine adjustments of $c^{(1)}=0.2-0.4$ in the problem considered here). For this reason, method 2 is not considered to be practical.

These results confirm that all of the Pareto optimal shapes for the two-dimensional problem considered here can be found using these methods except for method 2. They also indicate that the mean compliance in each case can be reduced depending on the weighting coefficient used.

4.2 Three-dimensional problem

Figure 13 shows a solid bracket, as an example of an application to a three-dimensional problem. Similar to the stress analysis of the two-dimensional problem, one end of the bracket was fully restrained and two different load distributions, a shear load $P^{(1)}$ and a tensile load $P^{(2)}$, were applied to the other end, as shown in Fig. 13(a). In the speed analysis, a sliding restriction around the periphery of the bracket was applied as a constraint, as indicated in Fig. 13(b). This condition allowed domain variation along the thickness of the bracket. Method 1 was
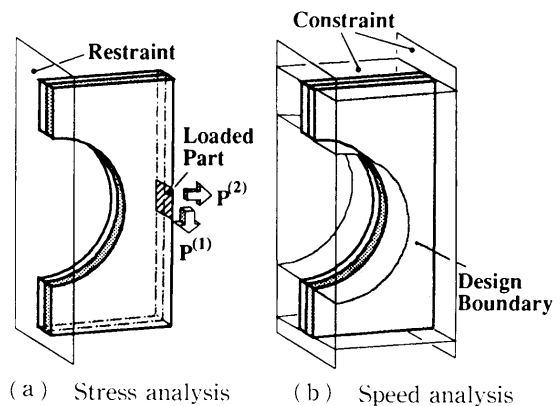

Fig. 11   Comparison of mean compliances

Fig. 12   Objective functional space

(a)   Stress analysis   (b)   Speed analysis

Fig. 13   Problem definition for solid bracket subject to multiloading in two directions
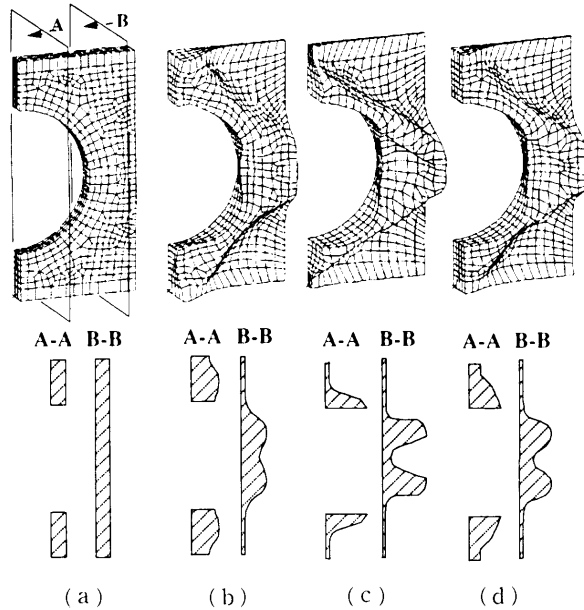
Fig. 14 Calculated results for solid bracket
(a) Initial shape
(b) Optimal shape for $P^{(1)}$
(c) Optimal shape for $P^{(2)}$
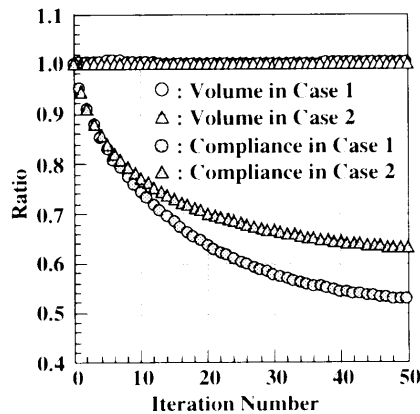(d) Pareto optimal shape ($c^{(1)} = 0.5$)

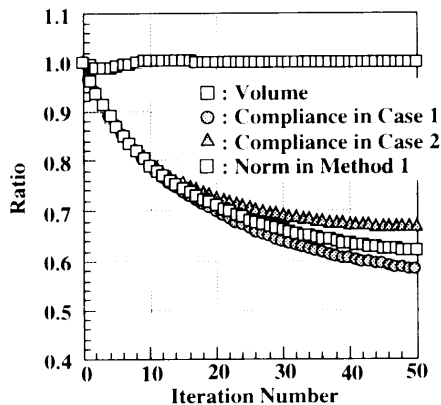Fig. 15 Iteration histories for single loading condition

Fig. 16 Iteration histories for method 1 under multiloading in two directions ($c^{(1)} = 0.5$)
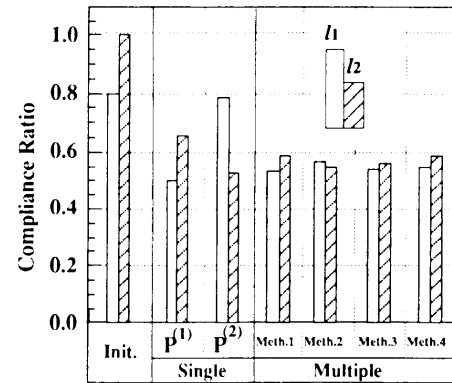

Fig. 17 Comparison of mean compliances

used and the weighting coefficient $c^{(1)}$ was set at 0.5. The numerical analysis was conducted using a symmetrical half model and a solid element with eight nodes.

Figure 14 shows the initial shape, the optimal shape obtained for each single load and the Pareto optimal shape. The Pareto optimal shape is intermediate between those for cases 1 and 2.

Optimization iteration histories for a single loading condition are shown in Fig. 15 and those for a multiple loading condition are shown in Fig. 16.

A comparison of the mean compliances obtained with the four methods is given in Fig. 17. All values were normalized to the mean compliance of the initial shape in case 2. The mean compliances obtained with the four methods show good agreement.

The results confirm that these techniques based on the traction method can also be used to find Pareto optimal shapes in three-dimensional problems.

5. Conclusions

We have described ways of applying the traction method to the mean compliance minimization of linear elastic continua subject to multiloading conditions, as are example of a multiobjective shape optimization problem. The objective functionals considered were scalarized using four representative norms. The effectiveness and practical utility of the proposed traction method were demonstrated in example applications to fundamental design problems.

References

(1) Haftka, R.T. and Grandhi, R.V., Structural Shape Optimization A Survey, Comput. Methods Appl. Mech. Eng., Vol. 57 (1986), p. 91.
(2) Ding, Y., Shape Optimization of Structures : A Literature Survey, Comput. Struct., Vol. 24, No. 6 (1986), p. 985.
(3) Stadler, W., Multicriteria Optimization in

Mechanics (A Survey), Appl. Mech. Rev., Vol. 37, No. 3 (1984), p. 277.

(4) Eschenauer, H., et al. (eds.), Multi Criteria Design Optimization, (1990), Springer Verlag, New York.

(5) Kosky, J. and Silvennoinen, R., Norm Methods and Partial Weighting in Multicriteria Optimization of Structures, Int. J. Num. Methods Eng., Vol. 24 (1987), p. 1101.

(6) Tada, Y., Seguchi, Y. and Yabu, T., Shape Determination Problem of Structures Considering Multiple Loading Conditions (Extension of Inverse Variational Shape Determination Method), Trans. Jpn. Soc. Mech. Engs., (in Japanese), Vol. 52, No. 473, A (1986), p. 233.

(7) Kikuchi, N., Optimal Design Theory Using the Homogenization Method, Industrial and Applied Mathematics., (in Japanese), Vol. 3, No. 1 (1993), p. 2.

(8) Azegami, H., A Solution to Domain Optimization Problems, Trans Jpn. Soc. Mech. Engs., (in Japanese), Vol. 60, No. 574, A (1994), p. 1479.

(9) Shimoda, M., Wu, Z., Azegami, H. and Sakurai, T., Numerical Method to Domain Optimization Problems Using a General Purpose FEM Code, Trans Jpn. Soc. Mech. Engs., (in Japanese), Vol. 60, No. 578, A (1994), p. 2418.

(10) For example, Sakawa, M., Optimization of Nonlinear Systems, (in Japanese), (1987), p. 125, Morikita Shuppan, Tokyo.

(11) Sokolowski, J. and Zolesio, J.P., Introduction to Shape Optimization, Shape Sensitivity Analysis, (1991), p. 7, Springer-Verlag, New York.

(12) Azegami, H. and Wu, Z., Trans Jpn. Soc. Mech. Engs., (in Japanese), Vol. 60, No. 578, A (1994), p. 2312.